Propagation of a filamentary femtosecond laser beam with high intensities at an air-solid interface

Zuoye Liu (刘作业)*, Yanghua Zhang (张杨华), Jingjie Ding (丁晶洁), Shaohua Sun (孙少华), and Bitao Hu (胡碧涛)**

School of Nuclear Science and Technology, Lanzhou University, Lanzhou 730000, China
**Corresponding author: zyl@lzu.edu.cn; **corresponding author: hubt@lzu.edu.cn*
Received August 24, 2016; accepted November 18, 2016; posted online December 27, 2016

The propagation of a filamentary laser beam at an air-glass surface is studied by setting the incident angle satisfying the total reflection condition. The images of the trajectory of the filamentary laser beam inside the sample and the output far-field spatial profiles are measured with varying incident laser pulse energies. Different from the general total reflection, a transmitted laser beam is detected along the propagation direction of the incident laser beam. The energy ratio of the transmitted laser beam depends on the pulse energies of the incident laser beam. The background energy reservoir surrounding the filament core can break the law of total reflection at the air-glass surface, resulting in the regeneration of the transmitted laser beam.

OCIS codes: 140.3440, 100.6640, 210.4770, 180.1790.
doi: 10.3788/COL201715.021401.

The self-guided propagation of intense femtosecond laser pulses in transparent media results in the generation of extended plasma channels that have exciting potential applications in the field of fundamental nonlinear optical physics[1–5]. A single and stable filament can be generated by using a conventional lens reaching a few tens of millimeters or even meters, if the laser intensity exceeds the critical power P_{cr}. Multifilaments will be formed as the incident pulse exceeding the critical power by an order of magnitude, which is unstable both in space and time[6]. Investigations on the characterization of a single filament with the incident laser power $P \geq P_{cr}$ and the interactions among multifilaments were performed to search for further applications of laser filamentation, e.g. amplified spontaneous emission air lasing in both the backward and forward directions[7,8]. Meanwhile, the propagation characteristics were also studied. Polynkin *et al.* experimentally observed the generation of curved plasma channels in both air and water by applying femtosecond Airy beams[9,10]. An extended and robust thermal waveguide structure in air with a lifetime of several milliseconds can be formed with femtosecond filaments[11], making possible the very-long-range guiding and distant projection of high-energy laser pulses and high average power beams.

However, the propagation characteristics of high power pulsed lasers at the interfaces of different transparent materials are ignored, particularly those of femtosecond filament. The air-glass surface is now widely used for the imaging of the lateral distribution of a filament[12–14]; however, the propagation characteristics are neglected. Setting the incident angle satisfying the total reflection condition, the propagation of a femtosecond filament at an air-glass surface is studied by showing the imaging of the propagation trajectory, the far-field profiles in this Letter. The dependence of the pulse energy of the reflective beam on the incident pulse energy is also measured.

Figure 1 shows the experimental setup. The basic parameters of the femtosecond laser beam are a pulse energy of 1.1 mJ, a central wavelength of 800 nm, a pulse duration of 60 fs, and a repetition rate of 1.0 kHz. One set of neutral density filters is applied to change the pulse energy of the incident beam. The beam size is reduced from 10 to 0.5 mm by a telescope. BK_7 glass is a hexahedral structure with two trapezoidal surfaces and four oblong surfaces; it is used as the sample. The angle is $\theta = 60^{\circ}$, and the laser beam is sent into the sample vertically in the measurement. The laser beam experiences filamentation inside the sample, and the incident angle of the filament on the upper air-glass surface is 60°. A telescope is set in front of a sensitive charge-coupled device camera (CCD2). It can collect and project plasma fluorescence into the sensitive area of CCD2, and a two-dimensional image of the propagation trajectories of the filamentary laser beam is measured. A fused silica lens and CCD1 with invariable space are applied to measure the output spatial profiles of the probe beam. Filter2 and CCD1 can be moved out of the beam pass, and an energy meter is applied to measure the laser pulse energy after the propagation in the sample.

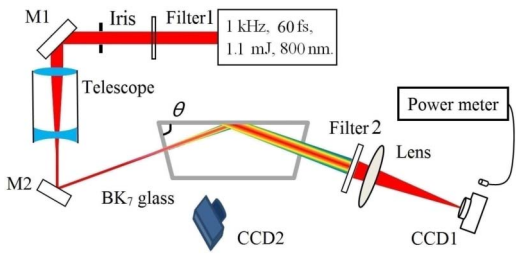

Fig. 1. Schematic layout of the experimental setup for studying the total reflection of a femtosecond filament at the air-glass surface. M1 and M2 are silver-coated mirrors.

According to the law of reflection, an 800 nm light beam propagating inside BK_7 glass will experience total reflection at the air-glass surface with an incident angle of 60° because the refractive index is $n_0 = 1.51$. In the experiment, a laser beam with a pulse energy of about 0.09 mJ is sent to form a filament inside the sample, corresponding to an input peak power $P \approx 660P_{cr}$, with the critical power for self-focusing defined as $P_{cr} = 3.77\lambda^2/(8\pi n_0 n_2)$, where λ is the center wavelength, and $n_2 = 3.18 \times 10^{-16}$ cm^2/W[15] is the nonlinear refractive index. During the propagation inside the glass, the laser beam forms a single stable filament. Figure 2(a) shows the propagation trajectory of the filamentary pulsed laser beam in the sample, which is imaged by the fluorescence of the plasma channel. After the reflection at the air-glass surface, the reflective filament passes through the glass vertically at the corresponding surface. The fluorescence intensity of the incident filament and reflective filament are in the same level, i.e., the plasma densities of both filaments are similar because they are closely related to the plasma fluorescence, the incident pulse energy. Changing the incident laser pulse energy to be 0.87 mJ, more than one filament are formed inside the glass, and it also experiences reflection at the air-glass surface, as illustrated by the propagation trajectory in Fig. 2(b). Two obvious filaments are found at the trajectory of the incident laser beam, while six separated filaments are found at different parts of the reflective trajectory. With further propagation of the laser beam, the beam's size increases slightly due to the interaction of the multifilaments, i.e., the distances among filaments increase with the propagation distance[16]. After the reflection at the air-glass surface, six separated filaments are formed at different parts of the trajectory of the reflective beam. From the number of the filaments formed at both sides, we can find that the air-glass surface changes the propagation characteristics of the laser beams a lot. Meanwhile, the fluorescence emission from the reflective filaments is weaker than that from the incident filaments.

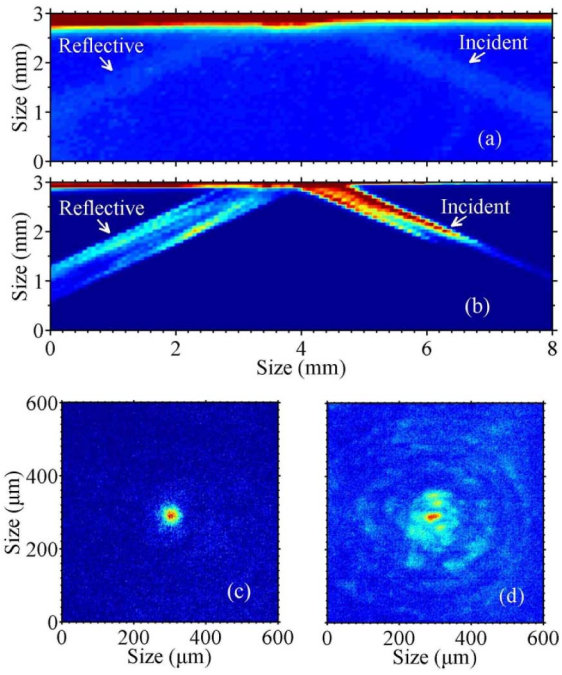

Fig. 2. Images of the propagation trajectory of the filamentary laser beams inside the BK_7 glass with the incident laser pulse energy set to be (a) 0.09 mJ and (b) 0.87 mJ. It should be pointed out that the hot tops in Figs. 2(a) and 2(b) are caused by the scattered light, which cannot totally blocked in the measurement. (c) and (d) are the corresponding far-field spatial profiles of the filamentary laser beams after reflection at the air-glass surface.

The far-field spatial profiles of the filamentary laser beam after reflection at the air-glass surface are also measured and illustrated in Figs. 2(c) and 2(d) for two different pulse energies. With the laser pulse energy set to 0.09 mJ, it presents as a self-cleaning core with symmetrical spatial distribution. The shape of the laser beam remains circular, which demonstrates that the air-solid surface is different from the air-liquid surface[17]. A laser beam with a low pulse energy can be deformed through total reflection at an air-water surface by inducing a convex mirror effect on the beam propagation[17]. The shape of the laser beam is a clear ellipse after total reflection at the air-water surface, and the intensity distribution remains Gaussian, while the laser beam is circular after reflection at a normal mirror. When the laser pulse energy is changed to 0.87 mJ, multifilaments are formed inside the glass. The far-field spatial profile of the reflective laser beam is displayed in Fig. 2(d).

By analyzing the supercontinuum generation during the laser filamentation in condensed media, Liu *et al.*[18] found the evidence for the clamping phenomenon, and the clamping intensity is believed to be ~10^{12} W/cm^2. Without thinking about the clamping effect, the peak laser intensity for a pulse energy of 0.09 mJ is $I_L = 5.6 \times 10^{12}$ W/cm^2, while that of 0.87 mJ is $I_H = 5.53 \times 10^{13}$ W/cm^2. As both of them are higher than the clamping intensity, it can be believed that the filamentary laser beam propagates inside the sample with the clamping intensity, which bring us to the question: How can a filamentary laser beam with such a high intensity be reflected by the air-glass surface?

Except for the reflective beam, a part of the laser beam transmits through the air-glass surface along the propagation direction of the incident laser beam presenting as the transmitted beam. With an incident pulse energy of 0.09 mJ, the pulse energy of the reflective laser beam is measured to be 0.05 mJ, i.e., 48% of the energy is lost to the transmitted beam by ignoring the energy loss due to the plasma generation. Because of the technical limitation, the far-field spatial profile of the transmitted beam is simply measured with a commercial camera by irradiating it on a white screen. It exhibits as an energy concentration center surrounding by conical emissions, as shown in Fig. 3(a). For the conical emission generated by a femtosecond laser filamentation inside a solid transparent medium, the far-field spatial profile appears as a white spot in the center surrounded by colored concentric

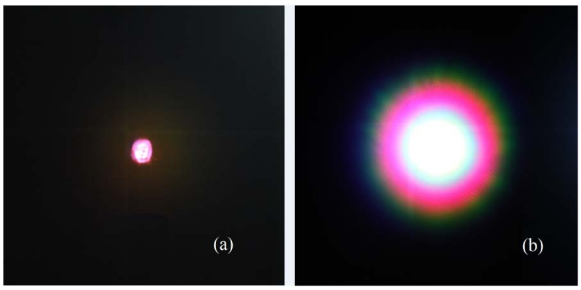

Fig. 3. Far-field spatial profile of the transmitted laser beam through the air-glass surface with the incident laser pulse energy set to be (a) 0.09 and (b) 0.87 mJ.

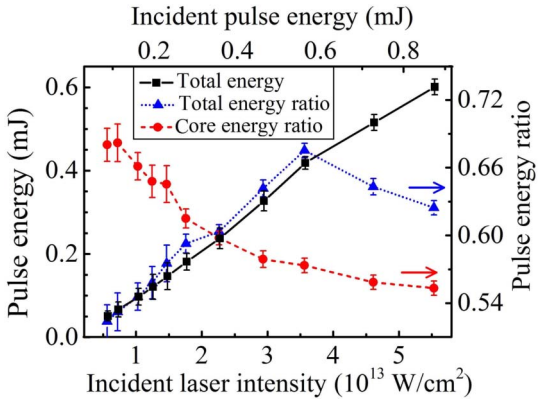

Fig. 4. Dependencies of the pulse energy of the reflective beam (the black solid line of squares), the total energy ratio, and the core energy ratio on the pulse energy of the incident laser beam.

rings, and the white spot is round and is where the energy is concentrated[16]. However, the shape of the spot shown in Fig. 3(a) is quasi-elliptic, and the conical emission is so weak that no obvious colored rings are detected. When the incident pulse energy is increased to be 0.78 mJ, 37.5% of the energy is taken by the transmitted laser beam, whose far-field spatial profile is shown in Fig. 3(b). The reflective index of the BK_7 glass experiences a wavelength dependence, which is larger than 1.50 with wavelengths shorter than 10^3 nm. With an incident angle of 60°, all the frequency components with wavelengths shorter than 10^3 nm will experience total reflection at the air-glass surface, which brings us to another question: How does part of the filamentary laser beam transmit through the air-glass surface?

In the propagation path of a filamentary laser beam, except for the bright cores corresponding to the filaments, a diffused illuminated area extending transversely around the filaments can also be observed, which is known as the background energy reservoir. The energy reservoir plays an important role in the processes of filament formation and regeneration[19]. It has been experimentally observed that filaments are regenerated when a central stopper blocks their propagation[20]. However, a filament will vanish at s short distance if its surrounding energy reservoir is blocked by an iris, and the distance depends on the size of the hole[21]. The filament itself contains only about 10% of the total energy, while most of the energy is located in the background energy reservoir. A special form of energy, the energy reservoir is not light and cannot be limited by the law of reflection. When a filamentary laser pulse arrives at the air-glass surface satisfying the total reflection condition, the filament cores, which contain frequency components from near-infrared to ultraviolet, can be totally reflected, while the background energy reservoir surrounding the filament experiences not only reflection but also transmission. The laser beam will be regenerated by the transmitted energy reservoir as illustrated by the far-field profile in Fig. 3. The amount of energy that can transmit through the air-glass surface depends on the incident laser pulse energy.

The dependence of the reflective pulse energy on the incident pulse energy (intensity) is illustrated by the black solid line of squares in Fig. 4. The reflective pulse energy exhibits an approximately linear change with the incident laser pulse energy. In order to quantify the relationship, we define the total (core) energy ratio as the measured reflective total (core) pulse energy divided by the incident pulse energy of the laser beam. The total energy ratio firstly increases from 52.4% to 67.5% by adjusting the incident laser pulse energy from 0.09 to 0.56 mJ, i.e., more and more energy saved in the background energy reservoir is reflected by the air-glass surface with the increase of the incident pulse energy. Then, it decreases from 67.5% to 62.5% with the further increase of the laser pulse energy from 0.56 to 0.87 mJ, which means more and more energy saved in the energy reservoir transmits through the air-glass surface.

Blocking the conical emission from the reflective beam, its core energy is measured, and the core energy ratio is shown by the red dashed line of circles in Fig. 4. It reduces from 18.0% to 5.3% with the increase of the incident laser intensity, i.e., more energy flows to the supercontinuum conical emission. Accompanied by the filamentation of a high-power laser pulse, various nonlinear processes are generated, and competitions among the supercontinuum conical emission, multifilamentation, and photon ionization during the filamentation process have been demonstrated[22–24], which is determined by the laser intensities. With the increase of the incident laser intensity, multifilamentation dominates during the filamentation process, and the interaction among multifilaments results in more intense nonlinear effects, such as self-phase modulation and self-steepening effect, which are significant for the conical emission. With the increase of the incident laser intensity, more and more energy is taken by the filament exhibiting as a supercontinuum conical emission instead of being saved in the background energy reservoir. The conical emission follows the law of reflection, and it is totally reflected by the air-glass surface. That is why the total energy ratio firstly increases with the incident laser intensity. With the further increase of the incident laser intensity, the supercontinuum conical emission reaches its maximum and relatively more energy is saved in the

background energy reservoir. More energy is taken by the transmitted laser beam, resulting in the decrease of the total energy ratio with the incident laser intensity.

Setting the incident angle satisfying the total reflection condition, we study the propagation of a filamentary pulse at an air-glass surface by showing the images of the propagation trajectories and the far-field profiles of the laser beams with different incident pulse energies. The experiment finds the filamentary laser beam experiences both reflection and transmission at the air-glass surface, while the transmitted laser pulse is regenerated by the background energy reservoir, which cannot be limited by the law of reflection as a special existence of energy. The ratio between the reflective beam and the transmitted beam depends on the incident laser pulse energy.

This work was supported by the National Natural Science Foundation of China (No. 11504148) and the Fundamental Research Funds for the Central Universities (Nos. lzujbky-2015-269 and lzujbky-2016-35).

References

1. A. Couairon and A. Mysyrowicz, Phys. Rep. **441**, 47 (2007).
2. J. Kasparian, M. Rodriguez, G. Mjean, J. Yu, E. Salmon, H. Wille, R. Bourayou, S. Frey, Y.-B. Andre, A. Mysyrowicz, R. Sauerbrey, J.-P. Wolf, and L. Woste, Science **301**, 61 (2003).
3. H.-R. Jiang, N. Yoshinaga, and M. Sano, Phys. Rev. Lett. **105**, 268302 (2010).
4. Z. Y. Liu, P. J. Ding, Y. C. Shi, X. Lu, Q. C. Liu, S. H. Sun, X. L. Liu, B. W. Ding, and B. T. Hu, Laser Phys. Lett. **9**, 649 (2012).
5. J. Wu, H. Cai, Y. Peng, Y. Q. Tong, A. Couairon, and H. P. Zeng, Laser Phys. **19**, 1759 (2009).
6. S. Birkholz, E. T. J. Nibbering, C. Bree, S. Skupin, A. Demircan, G. Genty, and G. Steinmeyer, Phys. Rev. Lett. **111**, 243903 (2013).
7. Y. Liu, P. Ding, G. Lambert, A. Houard, V. Tikhonchuk, and A. Mysyrowicz, Phys. Rev. Lett. **115**, 133203 (2015).
8. J. Yao, S. Jiang, W. Chu, B. Zeng, C. Wu, R. Lu, Z. Li, H. Xie, G. Li, C. Yu, Z. Wang, H. Jiang, Q. Gong, and Y. Cheng, Phys. Rev. Lett. **116**, 143007 (2016).
9. L. Bergé, S. Skupin, R. Nuter, J. Kasparian, and J.-P. Wolf, Rep. Prog. Phys. **70**, 1633 (2007).
10. P. Polynkin, M. Kolesik, J. V. Moloney, G. A. Siviloglou, and D. N. Christodoulides, Science **324**, 229 (2009).
11. N. Jhajj, E. W. Rosenthal, R. Birnbaum, J. K. Wahlstrand, and H. M. Milchberg, Phys. Rev. X **4**, 011027 (2014).
12. X. Yang, J. Wu, Y. Peng, Y. Tong, P. Lu, L. Ding, Z. Xu, and H. Zeng, Opt. Lett. **34**, 3806 (2009).
13. J. Yao, B. Zeng, W. Chu, J. Ni, and Y. Cheng, J. Mod. Opt. **59**, 245 (2012).
14. J. Liu, W. Li, H. Pan, and H. Zeng, Appl. Phys. Lett. **99**, 151105 (2011).
15. X. Lu, Q. Liu, Z. Liu, S. Sun, P. Ding, B. Ding, and B. Hu, Appl. Opt. **51**, 2045 (2012).
16. Z. Liu, X. Lu, Q. Liu, S. Sun, L. Li, X. Liu, B. Ding, and B. Hu, Appl. Phys. B **108**, 493 (2012).
17. O. Emile and J. Emile, Phys. Rev. Lett. **106**, 183904 (2011).
18. W. Liu, S. Petit, A. Becker, N. Akzbek, C. Bowden, and S. L. Chin, Opt. Commun. **202**, 189 (2002).
19. M. Mlejnek, E. M. Wright, and J. V. Moloney, Opt. Lett. **23**, 382 (1998).
20. A. Dubietis, E. Gaizauskas, G. Tamosauskas, and P. D. Trapani, Phys. Rev. Lett. **92**, 253903 (2004).
21. W. Liu, F. Theberge, E. Arevalo, J.-F. Gravel, A. Becker, and S. L. Chin, Opt. Lett. **30**, 2602 (2005).
22. H. Cai, J. Wu, X. Bai, H. Pan, and H. Zeng, Opt. Lett. **35**, 49 (2010).
23. L. Hong, Y. Hai, H. Yong, T. Ye, J. Jing, W. Cheng, and S. Jian, Chin. Opt. Lett. **13**, 033201 (2015).
24. H. L. Saadon, Chin. Opt. Lett. **13**, 071901 (2015).